J|A|C|S
COMMUNICATIONS

Published on Web 10/21/2004

In Situ Dual-Beam Coincidence Second Harmonic Generation as a Probe of Spatially Resolved Dynamics at Electrochemical Interfaces

Boguslaw Pozniak and Daniel A. Scherson*

Department of Chemistry, Case Western Reserve University, Cleveland, Ohio 44106-7078

Received May 29, 2004; E-mail: dxs16@po.cwru.edu

Adsorbed carbon monoxide on well-defined single-crystal metal surfaces may be regarded among the most widely studied systems in interfacial science.[1,2] Emphasis in the electrochemical community has focused by and large on CO adsorbed on well-defined Pt single-crystal surfaces in aqueous electrolytes. Of particular concern is to seek correlations between mode of bonding, reactivity, Pt surface microtopography, and applied potential, and rationalize the interplay of such structural and electronic factors within a quantum mechanical framework.[3] A better understanding of these aspects is expected to have an impact on the development and further optimization of electrocatalysts for reactions of relevance to technological devices, primarily fuel cells. Despite years of research, no concensus has been reached on certain fundamental characteristics of this system. In particular, two qualitatively different theoretical models for CO electrooxidation of Pt(111) surfaces in acid electrolytes have been found to yield remarkably good agreement with the temporal behavior of the measured current following application of a potential step, or chronocoulometric data: nucleation and growth, as proposed earlier by Love and Lipkowski,[4] and mean field approximation, as more recently advocated by Lebedeva et al.[5] The first of these models in based on the formation of adsorbed hydroxyl nuclei on (presumably) defect sites on Pt(111), which would promote oxidation of CO on neighboring sites via the reactant pair mechanism, opening new sites for further adsorption of hydroxyl to ensue. The islands thus formed will then grow via the reaction at the CO−hydroxyl boundary until the entire CO adlayer is oxidized. Implicit in this model is the lack of mobility of adsorbed CO along the surface. In stark contrast, the mean field model assumes the rates of migration of adsorbed CO to be higher than its electrooxidation rate to yield at all times an effective homogeneous surface. Because of their very nature, electrochemical methods rely on measurements of the *total* current flowing through the external circuit and, thus, are largely insensitive to spatial inhomogeneities. One possible approach to gain access to variations in coverage *along* the electrode surface and thereby help resolve this quandary is to use a spatially resolved technique endowed with sufficient specificity to distinguish areas with and without adsorbed CO. As shown originally by Lynch et al.,[6] adsorption of CO on Pt single crystals in electrochemical environments can elicit pronounced increases in the intensity of second harmonic generation (SHG), $I(2\omega)$, compared to the bare substrate over a wide potential range, providing ideal means for monitoring CO coverages as the reaction proceeds.

The present contribution describes the use of potential step−dual-beam coincidence SHG to probe simultaneously and with temporal resolution two different areas of a massive, well-defined Pt(111) surface (5 mm in diameter) in CO-saturated 0.1 M $HClO_4$ solutions. Two extreme situations can be envisioned: should the overall rate of CO oxidation be slower than surface diffusion, all areas of the electrode would, *at any specific time*, be compositionally identical (mean field approximation) and thus bring about qualitatively similar temporal variations in $I(2\omega)$ over the entire surface. If, in turn, the event(s) leading to CO oxidation, which may include random triggering, proceed at rates faster than diffusion, the temporal response of any two areas may not be identical (nucleation and growth).

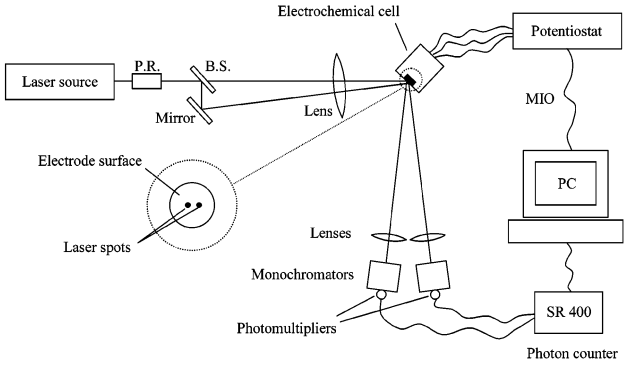

Figure 1. Schematic diagram for in situ dual-beam, coincidence SHG in electrochemical environments, where PR and BS refer to the polarizer and beam splitter. As described in the text, this instrumental array makes it possible to probe simultaneously and with temporal resolution two different areas of massive well-defined single-crystal electrodes.

The same in situ SHG experimental developed in this laboratory for single-beam measurements[7−9] was used for the dual-beam measurements described in this work, except that the primary excitation beam was split into two components, which were in turn focused on two different spots of the surface of a massive single-crystal Pt(111) specimen using a single lens (see Figure 1). As indicated herein, each of the reflected beams was then redirected to two independent filter/monochromator/ photomultiplier assemblies connected in turn to the inputs of a dual photon counter SR400 (Stanford Research Systems). The electrode potential was controlled by a potentiostat (PAR, model 173) and a universal programmer (PAR, model 175). At the beginning of the experiments, the electrode was polarized at a potential low enough for the c(2 × 2)-3CO adlayer to form on the Pt(111) surface, $E_{c(2\times2)}$, i.e., 30 mV vs RHE.[10] After a few seconds, the potential was stepped to a carefully selected value, $E_{CO(ox)}$, i.e., 870 mV, which was sufficiently low for the c(2 × 2)-3CO → $\sqrt{19} \times \sqrt{19}$ R23.4°-13CO phase transition to clearly precede electrooxidation of the entire adsorbed CO layer (see below). The electrode was then kept at $E_{CO(ox)}$ until the adsorbed CO present on the two probed areas on the Pt(111) surface was fully oxidized, and then stepped to $E_{c(2\times2)}$ to fully reconstitute the c(2 × 2)-3CO layer, at which point a new potential step was applied. For each of the runs, 10 or more consecutive of such forward and backward steps were applied, while recording simultaneously $I_{p,p}(2\omega)$ from each of the two spots, where p,p refers to the polarization states of the input (incident) and output (second harmonic), and also the current.

10.1021/ja046809j CCC: $27.50

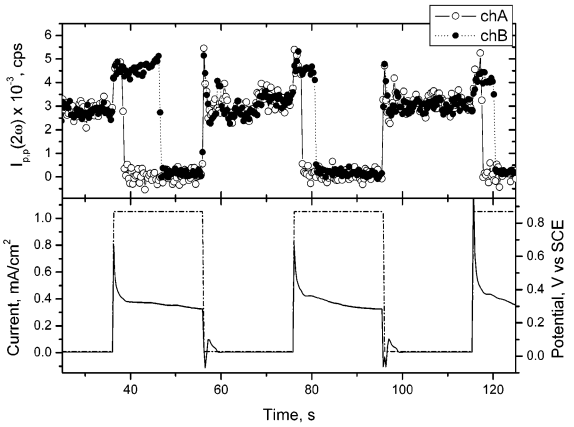

Figure 2. Plots of $I_{p,p}(2\omega)$ vs time acquired with the system in Figure 1 for a representative series of three consecutive double-potential-step sequences from 30 mV → 870 mV → 30 mV (see dash line in the lower panel in this figure), collected simultaneously from the two beams incident on two different areas on the Pt(111) surface (see empty and filled circles in the upper panel in this figure). The two spots in this case were separated by ca. 2 mm. The solid line in the lower panel in this figure represents the current response of the system to the potential perturbation (dashed lines) recorded simultaneously. Every point was acquired at intervals of 0.3 s.

Shown in the upper panel in Figure 2 are plots of $I_{p,p}(2\omega)$ vs time for a representative series of three consecutive double-potential-step sequences from 30 mV → 870 mV → 30 mV (see dashed line in the lower panel in this figure), collected simultaneously from the two beams incident on two different areas on the Pt(111) surface (see empty and filled circles in the upper panel in this figure) separated by ca. 2 mm. Cursory inspection of these traces reveals three characteristics common to all three sequences: the forward potential step, i.e., 30 mV → 870 mV, elicits a *simultaneous* and instantaneous increase in $I_{p,p}(2\omega)$ for both areas being probed. As reported originally by Akemann et al.,[11,12] such a large enhancement, ca. 55%, with respect to that observed for the c(2 × 2)-3CO adlayer at the lower potentials, is attributed to the formation of the $\sqrt{19} \times \sqrt{19}$ R23.4°-13CO phase. At longer times following this step, $I_{p,p}(2\omega)$ decreases in a rather sudden fashion to the same values found on Pt(111) at this potential in the strict absence of CO, signaling complete oxidation of adsorbed CO. Most significantly, the times at which full oxidation of the CO adlayer takes place are different on the two spots; i.e., the spot associated with the empty circles remains in the $\sqrt{19} \times \sqrt{19}$ R23.4°-13CO phase for a much longer period of time than that associated with the solid circles before undergoing electrooxidation. This provides rather unambiguous evidence that, under the conditions of these experiments, the interface is *temporally inhomogeneous* and thus that diffusion of adsorbed CO *along* the electrode surface is slower than the time constant observed (on the order a few seconds). Also noteworthy is the fact that the times at which electrooxidation of adsorbed CO is found to ensue on a single spot on the surface vary from sequence to sequence, suggesting that the process is stochastic rather than deterministic; i.e., the triggering of CO electrooxidation, under the conditions of these experiments, is not governed exclusively by the applied potential. The third common feature of all these sequences involves a large and very fast change in $I_{p,p}(2\omega)$ upon stepping the potential in the backward direction, i.e., 870 mV → 30 mV, followed by a much slower decrease until stabilization is achieved. This phenomenon is in all likelihood due to the adsorption of atomic hydrogen at the lower potential following application of the step, a virtually instantaneous process in the time scale shown, which is then replaced by CO on the surface at diffusion-controlled rates reaching values for $I_{p,p}(2\omega)$ characteristic of the c(2 × 2)-3CO adlayer. Strong support for this model is provided by the current response in the lower panel in this figure, which shows a negative spike at short times (electrosorption of hydrogen), followed by a positive peak, (CO adsorption/hydrogen displacement), and no net current thereafter, consistent with full formation of the c(2 × 2)-3CO adlayer. It is to be emphasized that the rapid rise in $I_{p,p}(2\omega)$ occurs simultaneously in both channels; hence, the differences in the overall temporal patterns observed are not due to instrumental artifacts. Furthermore, no significant differences were found between the current transients recorded during these experiments, a phenomenon that underscores the global nature of the electrochemical response, as opposed to the local character of the phenomena probed by the SHG.

As also shown by these data, electrooxidation of adsorbed CO for this rather small overpotential appears to be preceded by formation of a $\sqrt{19} \times \sqrt{19}$ R23.4°-13CO phase. This behavior is unlike that observed for measurements performed at much higher overpotentials involving Pt(111) faceted single-crystal microspheres, for which no evidence for the formation of the *dilute* phase was observed prior to CO electrooxidation. In fact, more recent experiments performed in our laboratory have provided evidence that the apparent rates of the (2 × 2)-3CO → $\sqrt{19} \times \sqrt{19}$ R23.4°-13CO phase transition as measured with SHG are on the order of a fraction of a second, which are orders of magnitude slower than those for the reverse transition.[9] It seems thus plausible that once a critical potential threshold is reached, electrooxidation can proceed directly from the (2 × 2)-3CO adlayer, i.e., faster than the phase transition would allow. Since the facets are believed to be atomically smooth, i.e., very low density of defects, in all likelihood oxidation begins at a nucleation just outside the facet and propagates from that point along the facet. Although the possibility does exist that more than one nucleation center could form and propagate during a single measurement, the probability of such an event appears highly unlikely.

In summary, the results presented in this work offer rather unambiguous proof that, for the conditions selected for these experiments, the rates at which adsorbed CO on Pt(111) undergo electrooxidation do depend on local surface properties, and, hence, that the diffusional rates of adsorbed CO cannot be assumed to be generally large enough as to render under all conditions the entire surface in an homogeneous state as invoked by the mean field approximation model.

Acknowledgment. This work was supported by a grant from the National Science Foundation.

References

(1) Iwasita, T.; Nart, F. C. *Prog. Surf. Sci.* **1997**, *55*, 271.
(2) Weaver, M. J.; Zou, S. In *Advances in Spectroscoy*; Clark, R. J. H., Hester, R. E., Eds., Wiley: Chichester, UK, 1998; Vol. 26.
(3) Wasileski, S. A.; Koper, M. T. M.; Weaver, M. J. *J. Am. Chem. Soc.* **2002**, *125*, 2796−2805 and references therein.
(4) Love, B.; Lipkowski, J. *ACS Symp. Ser.* **1988**, *378*, 484−496.
(5) Lebedeva, N. P.; Koper, M. T. M.; Feliu, J. M.; Santen, R. A. v. *J. Electroanal. Chem.* **2002**, *524*−*525*, 242−251.
(6) Lynch, M. L.; Barner, B. J.; Corn, R. M. *J. Electroanal. Chem.* **1991**, *300*, 447−465.
(7) Pozniak, B.; Mo, Y. B.; Stefan, I. C.; Mantey, K.; Hartmann, M.; Scherson, D. A. *J. Phys. Chem. B* **2001**, *105*, 7874−7877.
(8) Pozniak, B.; Mo, Y.; Scherson, D. A. *Faraday Discuss.* **2002**, *121*, 313−322.
(9) Pozniak, B.; Scherson, D. A. *J. Am. Chem. Soc.* **2003**, *125*, 7488−7489.
(10) Villegas, I.; Weaver, M. J. *J. Chem. Phys.* **1994**, *101*, 1648−1660.
(11) Akemann, W.; Friedrich, K. A.; Linke, U.; Stimming, U. *Surf. Sci.* **1998**, *404*, 571−575.
(12) Akemann, W.; Friedrich, K. A.; Stimming, U. *J. Chem. Phys.* **2000**, *113*, 6864−6874.

JA046809J